

See discussions, stats, and author profiles for this publication at: <https://www.researchgate.net/publication/230617052>

# Biofunctionalized Magnetic Nanoparticles for Specifically Detecting Biomarkers of Alzheimer's Disease in Vitro

ARTICLE in ACS CHEMICAL NEUROSCIENCE · SEPTEMBER 2011

Impact Factor: 4.36 · DOI: 10.1021/cn200028j · Source: PubMed

CITATIONS

20

READS

98

## 10 AUTHORS, INCLUDING:



**Shieh-Yueh Yang**

MagQu Co., Ltd.

34 PUBLICATIONS 259 CITATIONS

[SEE PROFILE](#)



**J. J. Chieh**

National Taiwan Normal University

67 PUBLICATIONS 653 CITATIONS

[SEE PROFILE](#)



**Ta-Fu Chen**

66 PUBLICATIONS 471 CITATIONS

[SEE PROFILE](#)



**Ming-Jang Chiu**

National Taiwan University

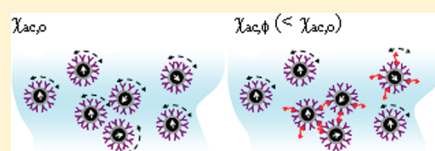
107 PUBLICATIONS 1,371 CITATIONS

[SEE PROFILE](#)

## Biofunctionalized Magnetic Nanoparticles for Specifically Detecting Biomarkers of Alzheimer's Disease in Vitro

Che-Chuan Yang,<sup>†</sup> Shieh-Yueh Yang,<sup>†,‡</sup> Jen-Jie Chieh,<sup>†</sup> Heng-Er Horng,<sup>\*,†</sup> Chin-Yih Hong,<sup>§</sup> Hong-Chang Yang,<sup>||</sup> K. H. Chen,<sup>†</sup> B. Y. Shih,<sup>†</sup> Ta-Fu Chen,<sup>⊥</sup> and Ming-Jang Chiu<sup>⊥,‡</sup><sup>†</sup>Institute of Electro-optical Science and Technology, National Taiwan Normal University, Taipei 116, Taiwan<sup>‡</sup>MagQu Co., Ltd., Sindian Dist., New Taipei City 231, Taiwan<sup>§</sup>Graduate Institute of Biomedical Engineering, National Chung-Hsing University, Taichung 402, Taiwan<sup>||</sup>Department of Physics, National Taiwan University, Taipei 106, Taiwan<sup>⊥</sup>Department of Neurology, National Taiwan University Hospital, College of Medicine, National Taiwan University, Taipei 104, Taiwan<sup>\*</sup>Department of Psychology, National Taiwan University, Taipei 106, Taiwan

**ABSTRACT:** Magnetic nanoparticles biofunctionalized with antibodies against  $\beta$ -amyloid-40 ( $A\beta$ -40) and  $A\beta$ -42, which are promising biomarkers related to Alzheimer's disease (AD), were synthesized. We characterized the size distribution, saturated magnetizations, and stability of the magnetic nanoparticles conjugated with anti- $A\beta$  antibody. In combination with immunomagnetic reduction technology, it is demonstrated such biofunctionalized magnetic nanoparticles are able to label  $A\beta$ s specifically. The ultralow-detection limits of assaying  $A\beta$ s in vitro using the magnetic nanoparticles via immunomagnetic reduction are determined to a concentration of  $\sim 10$  ppt (10 pg/mL). Further, immunomagnetic reduction signals of  $A\beta$ -40 and  $A\beta$ -42 in human plasma from normal samples and AD patients were analyzed, and the results showed a significant difference between these two groups. These results show the feasibility of using magnetic nanoparticles with  $A\beta$ s as reagents for assaying low-concentration  $A\beta$ s through immunomagnetic reduction, and also provide a promising new method for early diagnosis of Alzheimer's disease from human blood plasma.



**KEYWORDS:** Magnetic nanoparticles,  $\beta$ -amyloid, immunomagnetic reduction

Magnetic nanoparticles play a role in labeling biomolecules because of their transparent and nonquenched magnetic signals as well as their nanoscaled size. To achieve a specific labeling, specific bioprobes are conjugated onto magnetic nanoparticles. For example, to label a certain kind of protein, the antibodies against the protein are conjugated onto magnetic nanoparticles. With these features, biofunctionalized magnetic nanoparticles are applied as the contrast agent for magnetic resonance imaging,<sup>1,2</sup> sorters for target proteins or cells,<sup>3</sup> biomolecular markers, and so forth.

In the late 1900s, it was demonstrated biofunctionalized magnetic nanoparticles acted as markers to detect biomolecules.<sup>4</sup> By measuring the magnetic signals of magnetic nanoparticles which label target biomolecules, the concentration of the target biomolecules can be detected. Such technologies using biofunctionalized magnetic nanoparticles as labeling markers for assaying biomolecules are referred to as magnetically labeled immunoassay. Until now, several kinds of methods categorized in magnetically labeled immunoassay have been proposed, for example, measurement of saturated magnetization,<sup>5</sup> magnetic relaxation,<sup>4,6</sup> alternating-current magnetic susceptibility,<sup>7</sup> and magnetic remanence.<sup>8</sup> By utilizing these proposed methods, the magnetically labeled immunoassay has been demonstrated to be able to quantitatively detect not only proteins but also viruses, carcinogens, chemicals, and nucleic acids. In addition to

the versatility of the detected biomolecules, the magnetically labeled immunoassay shows such advantages as low interference by sample color, high accuracy, and low cost; there is a trend to use the magnetically labeled immunoassay in both the academic world and industry.

One of the important issues for the magnetically labeled immunoassay is the preparation of biofunctionalized magnetic nanoparticles. Depending on the to-be-detected biomolecules, magnetic nanoparticles are biofunctionalized with different bioprobes. In this work, concerning the globally growing problem of dementia diseases, the to-be-target biomolecules are focused on the biomarkers related to Alzheimer's disease. Although the biomarkers for Alzheimer's disease have not been definitively identified, the promising candidates are  $\beta$ -amyloids, especially  $\beta$ -amyloid-40 ( $A\beta$ -40) and  $\beta$ -amyloid-42 ( $A\beta$ -42), according to the reported papers.<sup>9–13</sup> Pathologically, excessive  $A\beta$ -40 and  $A\beta$ -42 in the cerebrospinal fluid (CSF) leads to the formation of plaques on the cortex, thus making brain activities dysfunctional. The  $A\beta$ -40/ $A\beta$ -42 plaques have been evidenced with target magnetic resonance imaging using biofunctionalized  $Fe_2O_3$  nanoparticles.<sup>14,15</sup>

**Received:** March 18, 2011

**Accepted:** May 30, 2011

**Published:** May 30, 2011

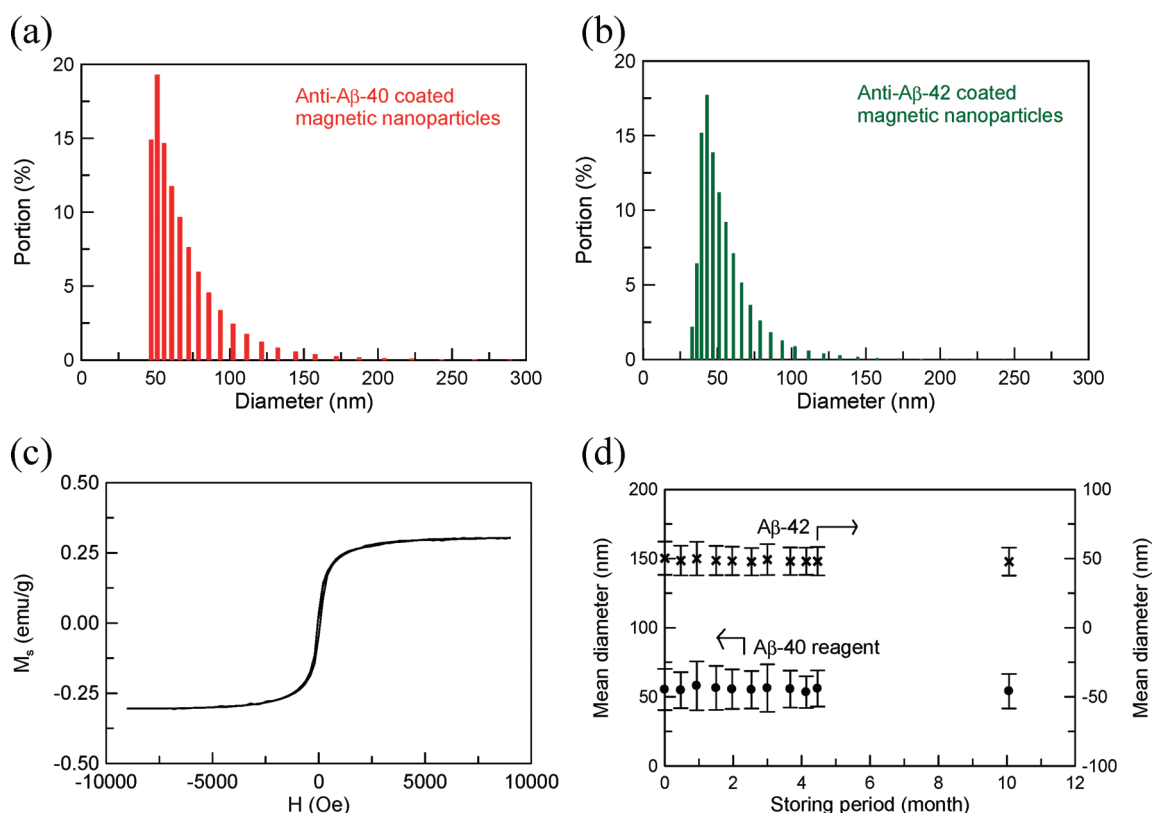


**Figure 1.** Size distributions of reagents (a)  $A\beta$ -40 and (b)  $A\beta$ -42, (c) magnetic hysteresis curve of reagent, and (d) the mean diameter of reagents as a function of the storage time at 2–8 °C.

Analysis of CSF  $A\beta$ -42 shows a significant reduction in AD patients compared to the control while  $A\beta$ -40 is unchanged or increased in AD.<sup>16</sup> Therefore, it has been suggested the  $A\beta$ -42/ $A\beta$ -40 ratio can improve AD diagnosis but others have not found these changes. However, the levels and significance of  $A\beta$  related proteins in plasma were more controversial.<sup>17</sup> Studies have shown plasma  $A\beta$ -42 and  $A\beta$ -40 levels can be elevated, reduced, or even unchanged in AD versus control patients.<sup>18,19</sup> The reasons plasma  $A\beta$ -42 levels are unstable are that the peptide is very sticky and binds to plasma proteins such as albumin, lipoproteins, and complement factors.<sup>20</sup> In addition, the effect of oligomerization of  $A\beta$ -42 on the measurement by enzyme-linked immunosorbent assay (ELISA) is unknown. Both the binding effect and oligomerization could mask  $A\beta$  epitopes and decrease the detectable levels. Therefore, we need a brand new method that can counter such nature of  $A\beta$ -42, to avoid the contradictory results shown in previous literature. The immunomagnetic reduction of the nanoparticles could be a potential solution.

It is quite inconvenient to diagnose Alzheimer's disease by traditional molecular detection (e.g., ELISA) of these two biomarkers from the cerebrospinal fluid. An easy and reliable molecule-diagnostic strategy, by testing blood plasma rather than cerebrospinal fluid, is now developing by combination of magnetic nanoparticles and immunomagnetic reduction technology.

To magnetically label  $A\beta$ -40 and  $A\beta$ -42, magnetic nanoparticles biofunctionalized with antibodies against  $A\beta$ -40 and  $A\beta$ -42 are synthesized in this work. The physical properties such as the particle size distribution, magnetism, and stability of magnetic nanoparticles dispersed in water are characterized. To investigate

the labeling of magnetic nanoparticles onto  $A\beta$ -40 and  $A\beta$ -42, properties such as a low-detection limit and interference via immunomagnetic reduction assay are examined. Preclinical tests have also been performed by testing plasma samples from normal and AD patients, to verify the feasibility of diagnosis of Alzheimer's disease according to immunomagnetic reduction signals.

## RESULTS AND DISCUSSION

The size distributions of the magnetic nanoparticles coated with anti- $A\beta$ -40 and anti- $A\beta$ -42 are shown in Figure 1a and b. The mean diameters of reagents  $A\beta$ -40 and  $A\beta$ -42 are 55.3 and 50.3 nm, respectively. Figure 1c plots the magnetic hysteresis curve for either of reagents  $A\beta$ -40 and  $A\beta$ -42. Clearly, the reagent displays superparamagnetism and the saturated magnetization is 0.3 emu/g (= 8.5 mg Fe/ml).

For the stability test, the mean diameters of reagents  $A\beta$ -40 and  $A\beta$ -42 are detected as a function of the storage time. Reagents  $A\beta$ -40 and  $A\beta$ -42 are stored at 2–8 °C. The results are shown in Figure 1d. Regardless of whether reagent  $A\beta$ -40 or  $A\beta$ -42 is used, there is no significant variation in the mean diameter when the reagents are stored at 2–8 °C for 10 months. This fact points to the high stability of reagents  $A\beta$ -40 and  $A\beta$ -42.

To observe the association between magnetic nanoparticles and to-be-detected  $A\beta$ s, the real-time  $\chi_{ac}$  signal, that is, the  $\chi_{ac}-t$  curve, of the mixture of reagent and sample solution is detected using a SQUID-based  $ac$  magnetosusceptometer (XacPro-S, MagQu). A typical  $\chi_{ac}-t$  curve is shown in Figure 2a for the mixture of reagent  $A\beta$ -40 and the 50 pg/mL  $A\beta$ -40 solution. The  $A\beta$ -40 solution is prepared by spiking  $A\beta$ -40 (H-1194, Bachem)

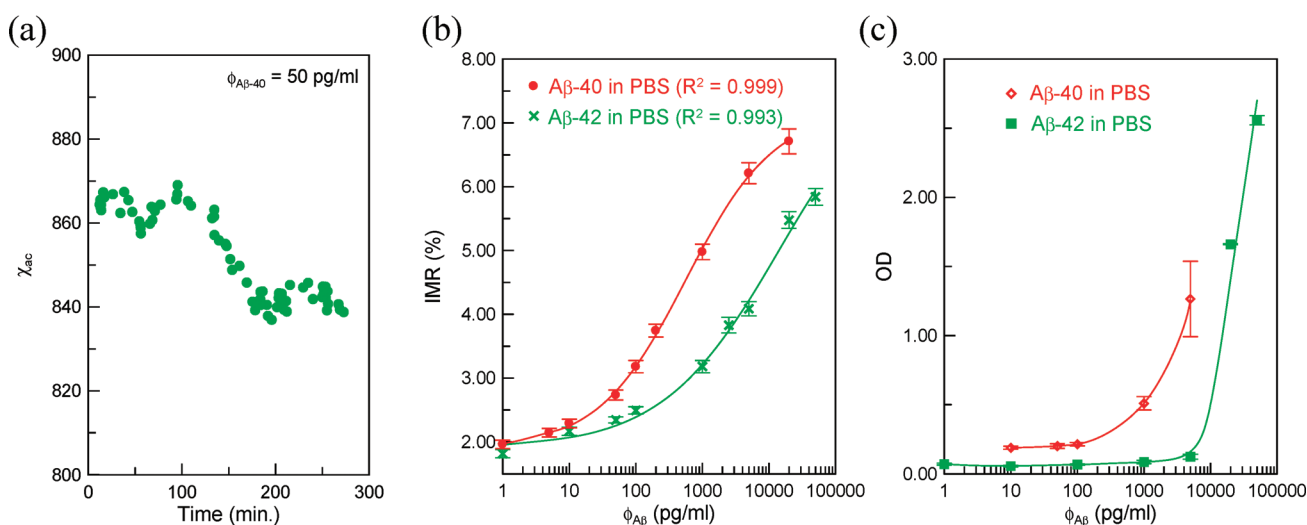


**Figure 2.** (a) Real-time  $\chi_{ac}$  signal of reagent mixed with to-be-detected sample, and A $\beta$ -concentration-dependent (b) IMR (%) via IMR and (c) optical density (OD) via ELISA.

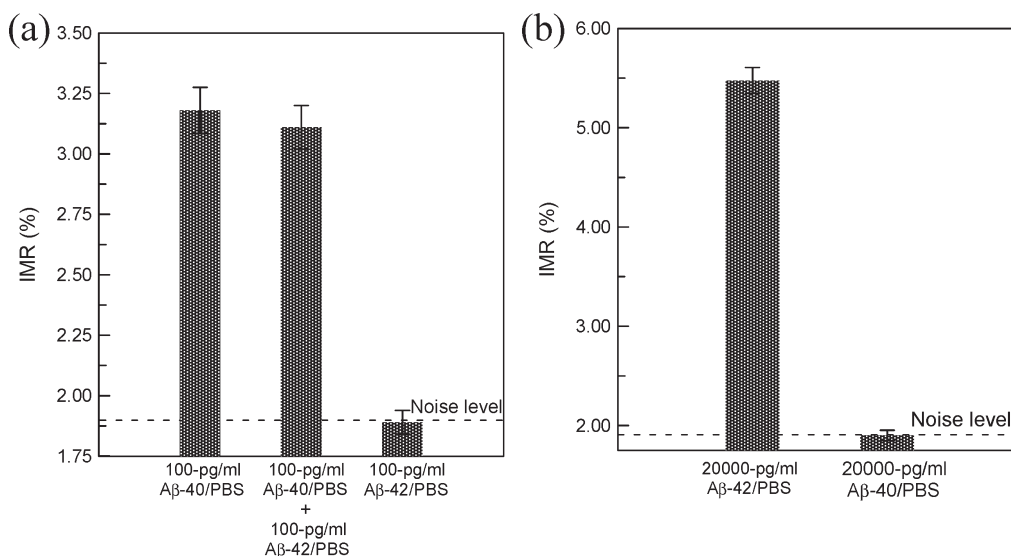


**Figure 3.** Interference tests for IMR assays on (a) A $\beta$ -40 and (b) A $\beta$ -42. In (a), reagent A $\beta$ -40 is used, and reagent A $\beta$ -42 is used in (b).

into pH 7.4 phosphate buffered saline (PBS) solution. In Figure 2a, at the beginning, the  $\chi_{ac}$  signal fluctuates around 865. At the time interval from 100 to 160 min, the  $\chi_{ac}$  signal descends. Then, the  $\chi_{ac}$  signal remains around 840. The higher-level  $\chi_{ac}$  signals at the time interval from 0 to 100 min correspond to the A $\beta$ -40 molecules not associated with magnetic nanoparticles. Once the A $\beta$ -40 molecules bind with the magnetic nanoparticles, the  $\chi_{ac}$  signal starts to decrease, as shown by the reduction in the  $\chi_{ac}$  signals at the time interval from 100 to 160 min. As the association between A $\beta$ -40 and magnetic nanoparticles finishes, the  $\chi_{ac}$  signal comes to an equilibrium level of lower values compared with that at the beginning. By averaging the data point at the time interval from 0 to 100 min, the mean value of the  $\chi_{ac}$  signals was found to be 862.6, and the mean value of  $\chi_{ac}$  signals beyond 160 min was obtained as 838.3. Thus, the reduction percentage in the  $\chi_{ac}$  signal, or so-called IMR signal, of the reagent–sample mixture is calculated to be 2.82%. With the

results of the triplicate tests, the IMR signal for 50 pg/mL A $\beta$ -40 solution using reagent A $\beta$ -40 was obtained as  $(2.73 \pm 0.08)\%$ .

The IMR signals for A $\beta$ -40 solutions of various concentrations were detected, and the results are shown with dot data points in Figure 2b. The detected concentration  $\phi_{A\beta}$  of A $\beta$ -40 PBS solution is from 1 to 20 000 pg/mL. It was found the IMR signal gently increases with increasing A $\beta$ -40 concentration from 1 to 50 pg/mL, followed by a marked increase in the IMR signal as the A $\beta$ -40 concentration increases to 5000 pg/mL, finally reaching a saturated value at an A $\beta$ -40 concentration higher than 10 000 pg/mL. Such behavior observed for the A $\beta$ -40 concentration dependent IMR signal shown in Figure 3 is very similar to the so-called logistic function

$$\text{IMR} (\%) = \frac{A - B}{1 + \left( \frac{\phi_{A\beta}}{\phi_o} \right)^{\gamma}} + B \quad (1)$$

where  $A$ ,  $B$ ,  $\varphi_0$ , and  $\gamma$  are the fitting parameters. The dot data points in Figure 2b are fitted with eq 1. The fitting curve is plotted together with the dot data points in Figure 2b. The parameters  $A$ ,  $B$ ,  $\varphi_0$ , and  $\gamma$  were found as 1.89, 7.20, 567.3, and 0.65, respectively. The correlation coefficient  $R^2$  between the rhombus points and the fitting curve is 0.999.

The fitting parameter  $A$  in eq 1 denotes the IMR signal as the concentration of  $A\beta$ -40 approaches zero. Therefore, the value of  $A$  corresponds to the noise level of the IMR signal for assaying  $A\beta$ -40. The noise is mainly attributed to the electric noise of SQUID ac magnetosusceptometer. Conventionally, the low-detection limit is defined as the concentration showing an IMR signal higher than the noise level by three times as the standard deviation of IMR signals for a low-concentration test. In this experiment, the standard deviation of low-concentration tests, say 10 pg/mL, is 0.07%. Thus, the low-detection limit is the concentration having an IMR signal of 2.1%. Via eq 1, the low-detection limit for assaying  $A\beta$ -40 is found to be 4.28 pg/mL.

As to  $A\beta$ -42, the IMR signal as a function of  $A\beta$ -42 using reagent  $A\beta$ -42 is examined. The experimental data are plotted with cross symbols in Figure 2b. These cross symbols are well fitted to eq 1 with fitting parameters  $A$  being 1.90,  $B$  being 8.10,  $\varphi_0$  being 14 157.7, and  $\gamma$  being 0.50. The standard deviation for a low-concentration test, say 10 pg/mL, is around 0.07%. Thus, the low-detection limit for assaying  $A\beta$ -42 is the concentration having an IMR signal of 2.11%. Using eq 1 with fitting parameters for  $A\beta$ -42, the low-detection limit for  $A\beta$ -42 is 16.40 pg/mL.

The results shown in Figure 2b are compared with that detected by ELISA. The protocols for detecting  $A\beta$ -40 and  $A\beta$ -42 are described in the user manuals of the ELISA kits (27718, IBL for  $A\beta$ -40; and KHB3441, Invitrogen for  $A\beta$ -42). The  $A\beta$ -40 concentration dependent optical densities (ODs) are also shown in Figure 2c with hollow tilted squares. It was found there is no significant difference in OD when the concentration of  $A\beta$ -40 is lower than 100 pg/mL. However, Figure 2b shows a clear difference in IMR signals between 10 and 1 pg/mL for  $A\beta$ -40. These results prove the low-detection limit in  $A\beta$ -40 concentration of IMR is lower than that of ELISA by 2 orders of magnitude.

The square points shown in Figure 2c denote the ODs for  $A\beta$ -42 solutions by using ELISA. The low-detection limit of ELISA for assaying  $A\beta$ -42 is around 105 pg/mL, while IMR measurement shows the low-detection limit to be 16.40 pg/mL. Therefore, SQUID-based IMR assay in  $A\beta$ -42 is more sensitive than ELISA by 4 orders of magnitude.

For real samples, such as cerebrospinal fluid or plasma,  $A\beta$ -40 and  $A\beta$ -42 coexist in samples. Since  $A\beta$ -40 is very similar to  $A\beta$ -42 in terms of molecular structures, the existing  $A\beta$ -42 might interfere with the association between  $A\beta$ -40 and anti- $A\beta$ -40 on the magnetic nanoparticles, or  $A\beta$ -40 could contribute a false-positive IMR signal when assaying  $A\beta$ -42 using reagent  $A\beta$ -42. It is necessary to examine the specificity of the associations between  $A\beta$ -40/ $A\beta$ -42 molecules and reagent  $A\beta$ -40/reagent  $A\beta$ -42. First, the interference from  $A\beta$ -42 to the assay of  $A\beta$ -40 using reagent  $A\beta$ -40 is examined. To do this, three samples are prepared. The first sample is the 100 pg/mL  $A\beta$ -40 PBS solution, the second sample is the mixture solution of 100 pg/mL  $A\beta$ -40 and 100-pg/mL  $A\beta$ -42 solution. The third sample is the 100 pg/mL  $A\beta$ -42 PBS solution. Using reagent  $A\beta$ -40, the IMR signals of these three samples are detected. The results are shown in Figure 3a. Clearly, there is a significant nondifference in the IMR signals for the first sample and the second sample. This

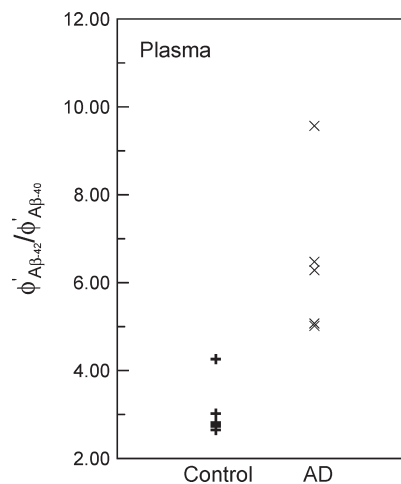


**Figure 4.** Values of parameter  $\phi'_{A\beta-42}/\phi'_{A\beta-40}$  in human plasma for control group (normal sample) and AD group (AD patients).

means the existence of  $A\beta$ -42 is not crucial to the assay for  $A\beta$ -40 using reagent  $A\beta$ -40. The IMR signal of the second sample resulted from  $A\beta$ -40, and it had nothing to do with  $A\beta$ -42. The independence of  $A\beta$ -42 in assaying  $A\beta$ -40 using reagent  $A\beta$ -40 is shown by the IMR signal of the third sample, which shows the noise level for the IMR signal.

In turn, the effect of  $A\beta$ -40 in detecting  $A\beta$ -42 using  $A\beta$ -42 is checked. Two samples consisting of 20 000 pg/mL  $A\beta$ -42 and 20 000 pg/mL  $A\beta$ -40 are prepared. The IMR signals for these two samples using reagent  $A\beta$ -42 are detected and shown in Figure 3b. The 20 000 pg/mL  $A\beta$ -42 sample shows a clear IMR signal around 5.5%, but no significant IMR signal can be found for the 20 000 pg/mL  $A\beta$ -40 sample. The results in Figure 3b reveal a high specificity of detecting  $A\beta$ -42 using reagent  $A\beta$ -42, even with the existence of  $A\beta$ -40.

The accuracy of diagnosing AD by assaying the concentrations of  $A\beta$ -40 and  $A\beta$ -42 in plasma is examined. Twelve human plasma samples are prepared. Six of the samples are from AD patients (AD group), and the other six samples are normal (control group). The human experiments were performed under regulations established by the Internal Review Board of National Taiwan University Hospital. For each sample, the IMR signals for  $A\beta$ -40 and  $A\beta$ -42 are detected by immunomagnetic reduction assay and using reagents  $A\beta$ -40 and  $A\beta$ -42. With the relationship in Figure 2b, the concentrations of  $A\beta$ -40 and  $A\beta$ -42 for each sample are obtained from IMR signals. The detected concentrations of  $A\beta$ -40 and  $A\beta$ -42 in plasma are denoted by  $\phi'_{A\beta-40}$  and  $\phi'_{A\beta-42}$ , respectively. In this work, the parameter  $\phi'_{A\beta-42}/\phi'_{A\beta-40}$  is used for investigating the diagnosing accuracy of AD. The values of the parameter for the control group are plotted with + symbols in Figure 4, and symbols  $\times$  are for the AD group. There is a clear difference in the parameter  $\phi'_{A\beta-42}/\phi'_{A\beta-40}$  between the control group and AD group. This preliminary result shows the feasibility of diagnosing AD by detecting the concentrations of  $A\beta$ -40 and  $A\beta$ -42 in plasma through immunomagnetic reduction assay.

In summary, magnetic reagents consisting of magnetic nanoparticles biofunctionalized with antibodies against  $A\beta$ -40 and  $A\beta$ -42 are synthesized. Through the immunomagnetic reduction assay, the abilities of the reagents associated with  $A\beta$ -40 at concentration levels lower than 10 pg/mL and  $A\beta$ -42 at



concentration levels lower than 20 pg/mL are demonstrated. Further, such reagents show high specificity to detect A $\beta$ -40 and A $\beta$ -42 using the IMR assay. These preliminary results of detecting the concentrations of A $\beta$ -40 and A $\beta$ -42 in human plasma show the promise of high-sensitivity and high-specificity diagnosis for Alzheimer's disease.

## METHODS

**Preparation of Magnetic Reagent.** The processes to synthesize magnetic Fe<sub>3</sub>O<sub>4</sub> nanoparticles are proposed by MagQu Co., Ltd. and are described in detail in refs 21 and 22. The solution consisting of a stoichiometric ratio, 1:2 ferrous sulfate heptahydrate (FeSO<sub>4</sub>·7H<sub>2</sub>O) and ferric chloride hexahydrate (FeCl<sub>3</sub>·6H<sub>2</sub>O), was mixed with an equal volume of aqueous dextran (molecular weight  $\sim$  100 000). Dextran formed a hydrophilic layer on the Fe<sub>3</sub>O<sub>4</sub> particles to disperse the particles in water. The mixture was heated to 70–90 °C and titrated with NH<sub>4</sub>OH solution to form black Fe<sub>3</sub>O<sub>4</sub> particles. Aggregates and excess unbound dextran were removed by centrifugation and gel filtration chromatography to obtain a concentrated magnetic fluid. The reagent with the desired magnetic concentration was obtained by diluting the concentrated magnetic fluid with pH 7.4 PBS solution.

To covalently bind antibodies, that is, anti-A $\beta$ -40 (sc-53822, Santa Cruz Biotech.) or anti-A $\beta$ -42 (437900, Invitrogen), to the dextran of the magnetic nanoparticles, 0.15 M NaIO<sub>4</sub> solution was added into the magnetic solution to oxidize dextran and create aldehyde groups (–CHO). Dextran reacts with antibodies via –CH=N–. Thus, the antibodies were covalently bound to dextran. Through magnetic separation, the unbound antibodies were separated from the magnetic solution. Hereafter, the magnetic solutions containing magnetic nanoparticles biofunctionalized with anti-A $\beta$ -40 and anti-A $\beta$ -42 are referred to as A $\beta$ -40 reagent and A $\beta$ -42 reagent, respectively.

### Size Distribution and Saturated Magnetization Analysis.

The size distribution of the magnetic nanoparticles and the magnetic concentration of reagents are characterized. Using dynamic laser scattering (Nanotracer-150, Microtrac), the size distribution of the magnetic nanoparticles biofunctionalized with antibodies was analyzed. The saturated magnetizations of the reagents are obtained by measuring the hysteresis curves at room temperature using a vibrating sample magnetometer (model 4500, EG&G). The maximum applied magnetic field is 9 kGauss.

**IMR Measurement.** The method to probe the association of to-be-detected A $\beta$ s and magnetic nanoparticles in reagents A $\beta$ -40 and A $\beta$ -42 is immunomagnetic reduction (IMR), which detects the reduction percentage in the alternating-current (ac) magnetic susceptibility  $\chi_{ac}$  of reagent due to the association of biofunctionalized magnetic nanoparticles and target biomolecules. The detailed mechanism of IMR is described in ref 23. In this work, the reduction percentage in  $\chi_{ac}$  of reagent is probed using the ac magnetosusceptometer (XacPro-S, MagQu) equipped with a high- $T_c$  superconducting-quantum-interference-device (SQUID) magnetometer as a magnetic sensor.

For examining the association between A $\beta$ s and biofunctionalized magnetic nanoparticles, 80  $\mu$ L/60- $\mu$ L A $\beta$ -40/A $\beta$ -42 reagent is mixed with a 40  $\mu$ L/60  $\mu$ L sample solution. The time-dependent  $\chi_{ac}$  signal of the mixture is recorded with the SQUID-based ac magnetosusceptometer. Once the magnetic nanoparticles bind with the A $\beta$  molecules, the  $\chi_{ac}$  signal of the mixture decreases. With the  $\chi_{ac}$  values at the initial and the end of the association of magnetic nanoparticles and A $\beta$  molecules, the reduction percentage of the  $\chi_{ac}$  signal for the sample is measured. In this paper, the reduction percentage in the  $\chi_{ac}$  signal is referred to as the IMR signal.

## AUTHOR INFORMATION

### Corresponding Author

\*E-mail: phyfv001@ntnu.edu.tw.

### Funding Sources

This work was supported by the National Science Council of Taiwan under Grant Numbers 98-2112-M-003-003, 98-2323-B-003-001-CC2, and NSC98-2752-M-002-016-PAE, by the Department of Health under Grant Numbers DOH98-TD-N-111-008 and DOH99-TD-N-111-008, and by the Ministry of Economic Affairs of Taiwan under Grant Numbers 1Z970688 (SBIR) and S09800226-203 (JAID).

### Author Contributions

C.-C.Y. and K.H.C. did the IMR measurements and data analysis for calculating the concentrations of A $\beta$ -40 and A $\beta$ -42. In addition, they performed the ELISA for A $\beta$ -40 and A $\beta$ -42. S.-Y.Y. and B.Y.S. synthesized magnetic particles as well as conjugated antibodies onto magnetic particles. H.-E.H., C.-Y.H., H.-C.Y., and J.-J.C. characterized the properties of magnetic particles with antibodies. For example, the measurements of magnetic hysteresis, particles size distribution, and so forth. T.-F.C. and M.-J.C. collected human plasma for the IMR assays on A $\beta$ -40 and A $\beta$ -42. Also, they provided medical information for assaying A $\beta$ -40 and A $\beta$ -42.

## REFERENCES

- (1) Roberts, D.; Zhu, W. L.; Frommen, C. M.; and Rosenzweig, Z. (2000) Synthesis of gadolinium oxide magnetoliposomes for magnetic resonance imaging. *J. Appl. Phys.* 87, 6208.
- (2) Wu, C. C.; Lin, L. Y.; Lin, L. C.; Huang, H. C.; Liu, Y. B.; Tsai, M. C.; Gao, Y. L.; Wang, W. C.; Yang, S. Y.; Horng, H. E.; Yang, H. C.; Tseng, W. K.; Lee, T. L.; Hsuan, C. F.; and Tseng, I. W. Y. (2008) Biofunctionalized magnetic nanoparticles for *in vitro* labeling and *in vivo* locating specific biomolecules. *Appl. Phys. Lett.* 92, 142504.
- (3) Inglis, D. W.; Riehn, R.; Sturm, J. C.; and Austin, R. H. (2006) Microfluidic high gradient magnetic cell separation. *J. Appl. Phys.* 99, 08K101.
- (4) Kötitz, R.; Weitschies, W.; Trahms, L.; Brewer, W.; and Semmler, W. J. (1999) Determination of the binding reaction between avidin and biotin by relaxation measurements of magnetic nanoparticles. *J. Magn. Mater.* 194, 62.
- (5) Horng, H. E.; Yang, S. Y.; Huang, Y. W.; Jiang, W. Q.; Hong, C. Y.; and Yang, H. C. (2005) Nanomagnetic particles for SQUID-based magnetically labeled immunoassay. *IEEE Trans. Appl. Supercond.* 15, 668.
- (6) Yang, H. C.; Yang, S. Y.; Liao, S. H.; Fang, G. L.; Huang, W. H.; Liu, C. H.; Horng, H. E.; and Hong, C. Y. (2006) Magnetic relaxation measurement in immunoassay using high-transition-temperature superconducting quantum interference device system. *J. Appl. Phys.* 99, 124701.
- (7) Krause, H. J.; Wolters, N.; Zhang, Y.; Offenhäusser, A.; Miethe, P.; Meyer, M. H. F.; Hartmann, M.; and Keusgen, M. (2007) Magnetic particle detection by frequency mixing for immunoassay applications. *J. Magn. Mater.* 311, 436.
- (8) Enpuku, K.; Kuroda, D.; Ohba, A.; Yang, T. Q.; Yoshinaga, K.; Nakahara, T.; Kuma, H.; and Hamasaki, N. (2003) Biological immunoassay utilizing magnetic marker and high- $T_c$  superconducting quantum interference device magnetometer. *Jpn. J. Appl. Phys.* 42, L1436.
- (9) Tapiola, T.; Alafuzoff, I.; Herukka, S. K.; Parkkinen, L.; Hartikainen, P.; Soininen, H.; and Pirttilä, T. (2009) Cerebrospinal fluid  $\beta$ -amyloid 42 and tau proteins as biomarkers of Alzheimer-type pathologic changes in the brain. *Arch. Neurol.* 66, 382.
- (10) Sobow, T.; Flirski, M.; Liberski, P. P.; and Kloszewska, I. (2007) Plasma A $\beta$  levels as predictors of response to rivastigmine treatment in Alzheimer's disease. *Acta Neurobiol. Exp.* 67, 131.

- (11) Fagan, A. M., Roe, C. M., Xiong, C., Mintun, M. A., Morris, J. C., and Holtzman, D. M. (2007) Cerebrospinal fluid tau/ $\beta$ -amyloid(42) ratio as a prediction of cognitive decline in nondemented older adults. *Arch. Neurol.* 64, 343.
- (12) Frankfort, S. V., Tulner, L. R., van Campen, J. P., Verbeek, M. M., Jansen, R. W., and Beijnen, J. H. (2008) Amyloid  $\beta$  protein and tau in cerebrospinal fluid and plasma as biomarkers for dementia: a review of recent literature. *Curr. Clin. Pharmacol.* 3, 123.
- (13) Blennow, K., Hampel, H., Weiner, M., and Zetterberg, H. (2010) Is it time for biomarker-based diagnostic criteria for prodromal Alzheimer's disease? *Nat. Rev. Neurol.* 6, 131.
- (14) Skaat, H., Sorci, M., Belfort, G., and Margel, S. (2008) Effect of maghemite nanoparticles on insulin amyloid fibril formation: Selective labeling, kinetics, and fibril removal by a magnetic field. *J. Biomed. Mater. Res., Part A* 91, 342.
- (15) Skaat, H., and Margel, S. (2009) Synthesis of fluorescent-maghemite nanoparticles as multimodal imaging agents for amyloid-beta fibrils detection and removal by a magnetic field. *Biochem. Biophys. Res. Commun.* 386, 645.
- (16) Humpel, C. (2010) Identifying and validating biomarkers for Alzheimer's disease. *Trends Biotechnol.* 29, 26.
- (17) Zetterberg, H., and Blennow, K. (2006) Plasma A $\beta$  in Alzheimer's disease--up or down? *Lancet Neurol.* 5, 638.
- (18) Cedazo-Mnguez, A., and Winblad, B. (2010) Biomarkers for Alzheimer's disease and other forms of dementia: clinical needs, limitations and future aspects. *Exp. Gerontol.* 45, 5.
- (19) Zetterberg, H., Blennow, K., and Hanse, E. (2010) Amyloid  $\beta$  and APP as biomarkers for Alzheimer's disease. *Exp. Gerontol.* 45, 23.
- (20) Irizarry, M. C. (2004) Biomarkers of Alzheimer disease in plasma. *NeuroRx* 1, 226.
- (21) Jiang, W., Yang, H. C., Yang, S. Y., Horng, H. E., Hung, J. C., Chen, Y. C., and Hong, C. Y. (2004) Preparation and properties of superparamagnetic nanoparticles with narrow size distribution and biocompatible. *J. Magn. Magn. Mater.* 283, 210.
- (22) Yang, S. Y., Jian, Z. F., Horng, H. E., Hong, C. Y., Yang, H. C., Wu, C. C., and Lee, Y. H. (2008) Dual immobilization and magnetic manipulation of magnetic nanoparticles. *J. Magn. Magn. Mater.* 320, 2688.
- (23) Chieh, J. J., Yang, S. Y., Jian, Z. F., Wang, W. C., Horng, H. E., Yang, H. C., and Hong, C. Y. (2008) Hyper-high-sensitivity wash-free magnetoreduction assay on biomolecules using high- $T_c$  superconducting quantum interference devices. *J. Appl. Phys.* 103, 14703.